

SUSY-QCD corrections to stop and sbottom decays into Higgs bosons

A. BARTL¹, H. EBERL², K. HIDAKA³,
S. KRAML², W. MAJEROTTO², W. POROD¹, Y. YAMADA⁴

(1) *Institut für Theoretische Physik, Universität Wien, A-1090 Vienna, Austria*

(2) *Institut für Hochenergiephysik, Österreichische Akademie der Wissenschaften,
A-1050 Vienna, Austria*

(3) *Department of Physics, Tokyo Gakugei University, Koganei, Tokyo 184-8501, Japan*

(4) *Department of Physics, Tohoku University, Sendai 980-8578, Japan*

Abstract

We calculate the $\mathcal{O}(\alpha_s)$ SUSY-QCD corrections to the widths of stop and sbottom decays into Higgs bosons within the Minimal Supersymmetric Standard Model. We give the complete analytical formulae paying particular attention to the on-shell renormalization of the soft SUSY-breaking parameters. We also perform a detailed numerical analysis of both stop and sbottom decays into all Higgs bosons h^0 , H^0 , A^0 , and H^\pm . We find that the SUSY-QCD corrections are significant, mostly negative and of the order of a few ten percent.

1 Introduction

Supersymmetry (SUSY) requires the existence of two scalar partners \tilde{q}_L and \tilde{q}_R to each quark q . In the case of the scalar partners of the top quark one expects a large mixing between \tilde{t}_L and \tilde{t}_R due to the large top quark mass [1]. The mixing of \tilde{b}_L and \tilde{b}_R may also be substantial if $\tan\beta = v_2/v_1$ is large (where v_1 and v_2 are the vacuum expectation values of the two Higgs doublets). Strong mixing induces large mass differences between the lighter mass eigenstate \tilde{q}_1 and the heavier one \tilde{q}_2 , $\tilde{q} = \tilde{t}$ or \tilde{b} . This implies in general a very complex decay pattern of

the heavier states. In addition to the “conventional” decays into neutralinos, charginos, and gluinos ($i, j = 1, 2; k = 1, \dots, 4$)

$$\tilde{t}_i \rightarrow t \tilde{\chi}_k^0, b \tilde{\chi}_j^+, \quad \tilde{b}_i \rightarrow b \tilde{\chi}_k^0, t \tilde{\chi}_j^-, \quad (1)$$

$$\tilde{t}_i \rightarrow t \tilde{g}, \quad \tilde{b}_i \rightarrow b \tilde{g}, \quad (2)$$

decays into vector bosons and Higgs particles can become kinematically possible ($i, j = 1, 2$):

$$\tilde{t}_2 \rightarrow \tilde{t}_1 Z^0, \quad \tilde{t}_i \rightarrow \tilde{b}_j W^+, \quad \tilde{b}_2 \rightarrow \tilde{b}_1 Z^0, \quad \tilde{b}_i \rightarrow \tilde{t}_j W^-, \quad (3)$$

$$\tilde{t}_2 \rightarrow \tilde{t}_1 (h^0, H^0, A^0), \quad \tilde{t}_i \rightarrow \tilde{b}_j H^+, \quad \tilde{b}_2 \rightarrow \tilde{b}_1 (h^0, H^0, A^0), \quad \tilde{b}_i \rightarrow \tilde{t}_j H^-. \quad (4)$$

All these squark decays were first discussed at tree-level in [2] within the Minimal Supersymmetric Standard Model (MSSM) [3]. A recent, more complete and systematic analysis of these decays at tree-level in [4] revealed that the bosonic decays of Eqs. (3) and (4) can be dominant in a wide range of the MSSM parameters due to the large Yukawa couplings and mixings of \tilde{t} and \tilde{b} . This could have an important impact on the search for \tilde{t}_2 and \tilde{b}_2 and the determination of the MSSM parameters at future colliders. Therefore it is important to study how SUSY-QCD corrections affect this tree-level result.

Within the last years SUSY-QCD corrections to a variety of processes were calculated. For the decays of Eq. (1) this was done in [5, 6, 7], for the decays Eq. (2) in [7, 8], and for the decays Eq. (3) in [9]. The SUSY-QCD corrections for the decays into Higgs bosons, Eq. (4), were briefly discussed in [10]. The QCD corrections to the related Higgs boson decays $(h^0, H^0, A^0) \rightarrow \tilde{q}_i \tilde{q}_j$ and $H^\pm \rightarrow \tilde{q}_i \tilde{q}'_j$ were calculated in [11, 10]. A thorough study of the corrections to the decays Eq. (4), including a detailed numerical analysis, is, however, still missing in the literature.

In this article we discuss the $\mathcal{O}(\alpha_s)$ SUSY-QCD corrections to the decay widths of Eq. (4) in the on-shell renormalization scheme within the MSSM. We give the complete formulas for these corrections and point out some subtleties which occur in the on-shell renormalization scheme. Whereas a numerical analysis was made only for $\tilde{t}_2 \rightarrow \tilde{t}_1 + (h^0, A^0)$ in [10], we perform a detailed analysis on stop and sbottom decays into all Higgs bosons h^0, H^0, A^0 , and H^\pm .

2 Tree-level formulae and notation

We first summarize the tree-level results and our notation. The squark mass matrix in the basis $(\tilde{q}_L, \tilde{q}_R)$ is given by [1]

$$\mathcal{M}_{\tilde{q}}^2 = \begin{pmatrix} m_{\tilde{q}_L}^2 & a_q m_q \\ a_q m_q & m_{\tilde{q}_R}^2 \end{pmatrix} = (\mathcal{R}^{\tilde{q}})^\dagger \begin{pmatrix} m_{\tilde{q}_1}^2 & 0 \\ 0 & m_{\tilde{q}_2}^2 \end{pmatrix} \mathcal{R}^{\tilde{q}} \quad (5)$$

with

$$m_{\tilde{q}_L}^2 = M_{\tilde{Q}}^2 + m_Z^2 \cos 2\beta (I_{3L}^q - e_q \sin^2 \theta_W) + m_q^2, \quad (6)$$

$$m_{\tilde{q}_R}^2 = M_{\{\tilde{U}, \tilde{D}\}}^2 + m_Z^2 \cos 2\beta e_q \sin^2 \theta_W + m_q^2, \quad (7)$$

$$a_q = A_q - \mu \{ \cot \beta, \tan \beta \} \quad (8)$$

for {up, down} type squarks. $M_{\tilde{Q},\tilde{U},\tilde{D}}$ and $A_{t,b}$ are soft SUSY–breaking parameters and μ is the Higgs mixing parameter in the superpotential. I_3^q and e_q are the third component of the weak isospin and the electric charge of the quark q . The squark mixing matrix $\mathcal{R}^{\tilde{q}}$ is

$$\mathcal{R}^{\tilde{q}} = \begin{pmatrix} \cos \theta_{\tilde{q}} & \sin \theta_{\tilde{q}} \\ -\sin \theta_{\tilde{q}} & \cos \theta_{\tilde{q}} \end{pmatrix} \quad (9)$$

with $0 \leq \theta_{\tilde{q}} < \pi$ by convention. The weak eigenstates \tilde{q}_L and \tilde{q}_R are related to their mass eigenstates \tilde{q}_1 and \tilde{q}_2 (with $m_{\tilde{q}_1} \leq m_{\tilde{q}_2}$) by

$$\begin{pmatrix} \tilde{q}_1 \\ \tilde{q}_2 \end{pmatrix} = \mathcal{R}^{\tilde{q}} \begin{pmatrix} \tilde{q}_L \\ \tilde{q}_R \end{pmatrix}. \quad (10)$$

In the $(\tilde{q}_1, \tilde{q}_2)$ basis the squark interaction with Higgs bosons $H_k = \{h^0, H^0, A^0, H^\pm\}$ can be written as $(i, j = 1, 2; k = 1 \dots 4; \alpha$ and β flavor indices)

$$\mathcal{L}_{\tilde{q}\tilde{q}H} = G_{ijk}^\alpha H_k^\dagger \tilde{q}_j^{\beta\dagger} \tilde{q}_i^\alpha. \quad (11)$$

The couplings G_{ijk}^α are

$$G_{ijk}^{\tilde{q}} = [\mathcal{R}^{\tilde{q}} \hat{G}_k^{\tilde{q}} (\mathcal{R}^{\tilde{q}})^T]_{ij} \quad (k = 1, 2, 3), \quad (12)$$

$$G_{ij4}^{\tilde{t}} = [\mathcal{R}^{\tilde{t}} \hat{G}_4 (\mathcal{R}^{\tilde{b}})^T]_{ij}, \quad G_{ij4}^{\tilde{b}} = [\mathcal{R}^{\tilde{b}} (\hat{G}_4)^T (\mathcal{R}^{\tilde{t}})^T]_{ij}, \quad (13)$$

with \hat{G}_k , $k = 1 \dots 4$, being the respective couplings in the $(\tilde{q}_L, \tilde{q}_R)$ basis as given in the Appendix. Note that $G_{ij4}^{\tilde{b}} = G_{ji4}^{\tilde{t}}$ and $G_{ij3}^{\tilde{q}} = [\hat{G}_3^{\tilde{q}}]_{ij}$. The tree–level width of the decay $\tilde{q}_i^\alpha \rightarrow \tilde{q}_j^\beta H_k$, Fig. 1a, is thus given by [2]

$$\Gamma^0(\tilde{q}_i^\alpha \rightarrow \tilde{q}_j^\beta H_k) = \frac{|G_{ijk}^\alpha|^2 \kappa(m_i^2, m_j^2, m_H^2)}{16\pi m_i^3} \quad (14)$$

where $m_i \equiv m_{\tilde{q}_i^\alpha}$, $m_j \equiv m_{\tilde{q}_j^\beta}$, $m_H \equiv m_{H_k}$, and $\kappa(x, y, z) = [(x - y - z)^2 - 4yz]^{1/2}$. For $k = 1, 2, 3$ we have of course $\alpha = \beta$ and $i = 2, j = 1$. For $k = 4$ we have $(\tilde{q}_i^\alpha, \tilde{q}_j^\beta) = (\tilde{t}_i, \tilde{b}_j)$ or $(\tilde{b}_i, \tilde{t}_j)$. In the following, we will omit flavor indices when possible (flavor = α if not given otherwise).

3 SUSY–QCD corrections

The $\mathcal{O}(\alpha_s)$ corrected decay amplitude in the on–shell renormalization scheme can be expressed as

$$G_{ijk}^{\text{corr}} = G_{ijk} + \delta G_{ijk}^{(v)} + \delta G_{ijk}^{(w)} + \delta G_{ijk}^{(c)} \quad (15)$$

where the superscript v denotes the vertex correction (Fig. 1b), w the squark wave–function correction (Fig. 1c), and c the counterterm due to the shift from the bare to the on–shell couplings. The $\mathcal{O}(\alpha_s)$ corrected decay width Γ is then given by

$$\Gamma = \Gamma^0 + \delta\Gamma^{(v)} + \delta\Gamma^{(w)} + \delta\Gamma^{(c)} + \delta\Gamma_{\text{real}} \quad (16)$$

with

$$\delta\Gamma^{(a)} = \frac{\kappa(m_i^2, m_j^2, m_H^2)}{8\pi m_i^3} \operatorname{Re} \left\{ G_{ijk}^* \delta G_{ijk}^{(a)} \right\} \quad (a = v, w, c) \quad (17)$$

and $\delta\Gamma_{real}$ the correction due to real gluon emission (Fig. 1e) which has to be included in order to cancel the infrared divergences. We use dimensional reduction [12] as regularization scheme. Analogous calculations were performed for the crossed channels of Higgs decays into squarks in [11, 10].

3.1 Vertex corrections

The vertex correction due to the gluon–squark–squark loop in Fig. 1b is

$$\delta G_{ijk}^{(v,g)} = \frac{\alpha_s}{3\pi} G_{ijk} \left[B_0(m_i^2, 0, m_i^2) + B_0(m_j^2, 0, m_j^2) - B_0(m_{H_k}^2, m_i^2, m_j^2) + 2X C_0 \right] \quad (18)$$

with $X = m_i^2 + m_j^2 - m_{H_k}^2$. B_0 and C_0 are the standard two- and three-point functions [13] for which we follow the conventions of [14]. In this case, $C_0 = C_0(m_i^2, m_{H_k}^2, m_j^2; \lambda^2, m_i^2, m_j^2)$. As usual, we introduce a gluon mass λ to regularize the infrared divergence.

The graph with the gluino–quark–quark loop in Fig. 1b leads to

$$\delta G_{21\ell}^{(v,\tilde{g})} = -\frac{2}{3} \frac{\alpha_s}{\pi} m_{\tilde{g}} \cos 2\theta_{\tilde{q}} s_\ell^\alpha \left[B_0(m_{\tilde{q}_2}^2, m_{\tilde{g}}^2, m_q^2) + B_0(m_{\tilde{q}_1}^2, m_{\tilde{g}}^2, m_q^2) + (4m_q^2 - m_{H_\ell}^2) C_0 \right] \quad (19)$$

for the decays into h^0 and H^0 ($\ell = 1, 2$),

$$\begin{aligned} \delta G_{213}^{(v,\tilde{g})} = & -\frac{2}{3} \frac{\alpha_s}{\pi} s_3^\alpha \left\{ m_q \sin 2\theta_{\tilde{q}} \left[B_0(m_{\tilde{q}_2}^2, m_{\tilde{g}}^2, m_q^2) - B_0(m_{\tilde{q}_1}^2, m_{\tilde{g}}^2, m_q^2) + (m_{\tilde{q}_2}^2 - m_{\tilde{q}_1}^2) C_0 \right] \right. \\ & \left. + m_{\tilde{g}} \left[B_0(m_{\tilde{q}_2}^2, m_{\tilde{g}}^2, m_q^2) + B_0(m_{\tilde{q}_1}^2, m_{\tilde{g}}^2, m_q^2) - m_A^2 C_0 \right] \right\}, \quad (20) \end{aligned}$$

for the decay into A^0 , and

$$\begin{aligned} \delta G_{ij4}^{(v,\tilde{g})} = & \frac{2}{3} \frac{\alpha_s}{\pi} \left\{ \left[(m_{q^\alpha} A_{11} + m_{q^\beta} A_{22}) s_4^\alpha + (m_{q^\alpha} A_{22} + m_{q^\beta} A_{11}) s_4^\beta \right] B_0(m_{H^+}^2, m_t^2, m_b^2) \right. \\ & + \left[(m_{q^\alpha} A_{11} - m_{\tilde{g}} A_{21}) s_4^\alpha + (m_{q^\alpha} A_{22} - m_{\tilde{g}} A_{12}) s_4^\beta \right] B_0(m_i^2, m_{\tilde{g}}^2, m_{q^\alpha}^2) \\ & + \left[(m_{q^\beta} A_{22} - m_{\tilde{g}} A_{21}) s_4^\alpha + (m_{q^\beta} A_{11} - m_{\tilde{g}} A_{12}) s_4^\beta \right] B_0(m_j^2, m_{\tilde{g}}^2, m_{q^\beta}^2) \\ & + \left[m_{q^\beta} (m_{q^\alpha}^2 - m_i^2 + m_{\tilde{g}}^2) (A_{22} s_4^\alpha + A_{11} s_4^\beta) \right. \\ & \quad + m_{q^\alpha} (m_{q^\beta}^2 - m_j^2 + m_{\tilde{g}}^2) (A_{11} s_4^\alpha + A_{22} s_4^\beta) \\ & \quad + m_{\tilde{g}} (m_{H^+}^2 - m_{q^\alpha}^2 - m_{q^\beta}^2) (A_{21} s_4^\alpha + A_{12} s_4^\beta) \\ & \quad \left. - 2m_{\tilde{g}} m_{q^\alpha} m_{q^\beta} (A_{12} s_4^\alpha + A_{21} s_4^\beta) \right] C_0 \left. \right\} \quad (21) \end{aligned}$$

with $A_{nm} = \mathcal{R}_{in}^\alpha \mathcal{R}_{jm}^\beta$ for the decay into a charged Higgs boson.

In Eqs. (19) to (21) $C_0 = C_0(m_i^2, m_{H_k}^2, m_j^2; m_{\tilde{g}}^2, m_{q^\alpha}^2, m_{q^\beta}^2)$; s_k^q are the Higgs couplings to quarks:

$$\mathcal{L}_{qqH} = s_1^q h^0 \bar{q} q + s_2^q H^0 \bar{q} q + s_3^q A^0 \bar{q} \gamma^5 q + H^+ \bar{t} (s_4^b P_R + s_4^t P_L) b + H^- \bar{b} (s_4^t P_R + s_4^b P_L) t \quad (22)$$

with

$$\begin{aligned} s_1^t &= -\frac{g m_t}{2 m_W \sin \beta} \cos \alpha, & s_2^t &= -\frac{g m_t}{2 m_W \sin \beta} \sin \alpha, & s_3^t &= i \frac{g m_t}{2 m_W} \cot \beta, & s_4^t &= \frac{g m_t}{\sqrt{2} m_W} \cot \beta, \\ s_1^b &= \frac{g m_b}{2 m_W \cos \beta} \sin \alpha, & s_2^b &= -\frac{g m_b}{2 m_W \cos \beta} \cos \alpha, & s_3^b &= i \frac{g m_b}{2 m_W} \tan \beta, & s_4^b &= \frac{g m_b}{\sqrt{2} m_W} \tan \beta. \end{aligned} \quad (23)$$

The vertex correction due to the four-squark interaction in Fig. 1b is

$$\delta G_{ijk}^{(v, \tilde{q})} = -\frac{\alpha_s}{3\pi} \sum_{n,m=1,2} \mathcal{S}_{in}^\alpha \mathcal{S}_{jm}^\beta G_{nmk} B_0(m_{H_k}^2, m_{\tilde{q}_m}^2, m_{\tilde{q}_n}^2) \quad (24)$$

with

$$\mathcal{S}_{in}^\alpha = \begin{pmatrix} \cos 2\theta_{\tilde{q}} & -\sin 2\theta_{\tilde{q}} \\ -\sin 2\theta_{\tilde{q}} & -\cos 2\theta_{\tilde{q}} \end{pmatrix}_{in}^\alpha \quad (25)$$

3.2 Wave-function correction

The wave-function correction is

$$\delta G_{ijk}^{(w)} = \frac{1}{2} \left[\delta \tilde{Z}_{ii}^\alpha + \delta \tilde{Z}_{jj}^\beta \right] G_{ijk}^\alpha + \delta \tilde{Z}_{i'i}^\alpha G_{i'jk}^\alpha + \delta \tilde{Z}_{j'j}^\beta G_{ij'k}^\alpha, \quad \begin{matrix} i \neq i' \\ j \neq j' \end{matrix} \quad (26)$$

where the \tilde{Z}_{nm}^α are the squark wave-function renormalization constants for \tilde{q}^α . They stem from the gluon, gluino, and squark loops of Fig. 1c¹ and are given by:

$$\delta \tilde{Z}_{nn}^{(g, \tilde{g})} = -\text{Re} \left\{ \dot{\Sigma}_{nn}^{(g, \tilde{g})}(m_{\tilde{q}_n}^2) \right\}, \quad \delta \tilde{Z}_{n'n}^{(\tilde{g}, \tilde{q})} = \frac{\text{Re} \left\{ \dot{\Sigma}_{n'n}^{(\tilde{g}, \tilde{q})}(m_{\tilde{q}_n}^2) \right\}}{m_{\tilde{q}_{n'}}^2 - m_{\tilde{q}_n}^2}, \quad n \neq n' \quad (27)$$

with $\dot{\Sigma}_{nn}(m^2) = \partial \Sigma_{nn}(p^2) / \partial p^2 |_{p^2=m^2}$. The contribution due to gluon exchange is

$$\dot{\Sigma}_{nn}^{(g)}(m_{\tilde{q}_n}^2) = -\frac{2}{3} \frac{\alpha_s}{\pi} \left[B_0(m_{\tilde{q}_n}^2, 0, m_{\tilde{q}_n}^2) + 2m_{\tilde{q}_n}^2 \dot{B}_0(m_{\tilde{q}_n}^2, \lambda^2, m_{\tilde{q}_n}^2) \right], \quad (28)$$

and those due to gluino exchange are

$$\begin{aligned} \dot{\Sigma}_{nn}^{(\tilde{g})}(m_{\tilde{q}_n}^2) &= \frac{2}{3} \frac{\alpha_s}{\pi} \left[B_0(m_{\tilde{q}_n}^2, m_{\tilde{g}}^2, m_q^2) + (m_{\tilde{q}_n}^2 - m_q^2 - m_{\tilde{g}}^2) \dot{B}_0(m_{\tilde{q}_n}^2, m_{\tilde{g}}^2, m_q^2) \right. \\ &\quad \left. - 2m_q m_{\tilde{g}} (-1)^n \sin 2\theta_{\tilde{q}} \dot{B}_0(m_{\tilde{q}_n}^2, m_{\tilde{g}}^2, m_q^2) \right], \end{aligned} \quad (29)$$

$$\Sigma_{12}^{(\tilde{g})}(m_{\tilde{q}_n}^2) = \Sigma_{21}^{(\tilde{g})}(m_{\tilde{q}_n}^2) = \frac{4}{3} \frac{\alpha_s}{\pi} m_{\tilde{g}} m_q \cos 2\theta_{\tilde{q}} B_0(m_{\tilde{q}_n}^2, m_{\tilde{g}}^2, m_q^2). \quad (30)$$

The four-squark interaction gives

$$\Sigma_{12}^{(\tilde{q})}(m_{\tilde{q}_n}^2) = \Sigma_{21}^{(\tilde{q})}(m_{\tilde{q}_n}^2) = \frac{\alpha_s}{6\pi} \sin 4\theta_{\tilde{q}} \left[A_0(m_{\tilde{q}_2}^2) - A_0(m_{\tilde{q}_1}^2) \right] \quad (31)$$

where $A_0(m^2)$ is the standard one-point function in the convention of [14].

¹The gluon loop due to the $\tilde{q}\tilde{q}gg$ interaction gives no contribution because it is proportional to $\lambda^2 \ln \lambda \rightarrow 0$.

3.3 Shift from bare to on-shell parameters

We next fix the shift from the bare to the on-shell couplings $\delta G_{ijk}^{(c)}$ in Eq. (15). We follow the procedure which was first given in [11]. From Eqs. (12) and (9) we get for the squark decays into h^0 or H^0 ($\ell = 1, 2$)

$$\begin{aligned}\delta G_{21\ell}^{\tilde{q}(c)} &= \left[\mathcal{R}^{\tilde{q}} \delta \hat{G}_\ell^{\tilde{q}} (\mathcal{R}^{\tilde{q}})^T + \delta \mathcal{R}^{\tilde{q}} \hat{G}_\ell^{\tilde{q}} (\mathcal{R}^{\tilde{q}})^T + \mathcal{R}^{\tilde{q}} \hat{G}_\ell^{\tilde{q}} \delta (\mathcal{R}^{\tilde{q}})^T \right]_{21} \\ &= \cos 2\theta_{\tilde{q}} \left[\delta \hat{G}_\ell^{\tilde{q}} \right]_{21} - (G_{11\ell}^{\tilde{q}} - G_{22\ell}^{\tilde{q}}) \delta \theta_{\tilde{q}}\end{aligned}\quad (32)$$

with $\delta \hat{G}_\ell^{\tilde{q}}$ obtained by varying Eqs. (52–54), e. g.

$$\delta \hat{G}_2^{\tilde{t}} = -\frac{g}{2m_W s_\beta} \begin{pmatrix} 4m_t s_\alpha \delta m_t & \delta(m_t A_t) s_\alpha - \mu c_\alpha \delta m_t \\ \delta(m_t A_t) s_\alpha - \mu c_\alpha \delta m_t & 4m_t s_\alpha \delta m_t \end{pmatrix}, \quad (33)$$

$$\delta \hat{G}_2^{\tilde{b}} = -\frac{g}{2m_W c_\beta} \begin{pmatrix} 4m_b c_\alpha \delta m_b & \delta(m_b A_b) c_\alpha - \mu s_\alpha \delta m_b \\ \delta(m_b A_b) c_\alpha - \mu s_\alpha \delta m_b & 4m_b c_\alpha \delta m_b \end{pmatrix} \quad (34)$$

with $s_\beta = \sin \beta$, $c_\beta = \cos \beta$, $s_\alpha = \sin \alpha$, $c_\alpha = \cos \alpha$, and α the Higgs mixing angle. $\delta \hat{G}_1^{\tilde{q}}$ is obtained from Eqs. (33) and (34) by:

$$\delta \hat{G}_1^{\tilde{q}} = \left(\delta \hat{G}_2^{\tilde{q}} \text{ with } \alpha \rightarrow \alpha + \pi/2 \right). \quad (35)$$

For the couplings to the A^0 boson we have explicitly

$$\delta G_{213}^{\tilde{q}(c)} = \frac{ig}{2m_W} \left[\delta(m_q A_q) \{ \cot \beta, \tan \beta \} + \mu \delta m_q \right], \quad (36)$$

where $\cot \beta$ ($\tan \beta$) is for $\tilde{q} = \tilde{t}$ (\tilde{b}).

For the decay $\tilde{t}_i \rightarrow \tilde{b}_j H^+$ ($k = 4$) we get

$$\delta G_{ij4}^{\tilde{t}(c)} = \left[\mathcal{R}^{\tilde{t}} \delta \hat{G}_4 (\mathcal{R}^{\tilde{b}})^T \right]_{ij} - (-1)^i G_{i'j4}^{\tilde{t}} \delta \theta_{\tilde{t}} - (-1)^j G_{ij'4}^{\tilde{t}} \delta \theta_{\tilde{b}}, \quad \begin{matrix} i \neq i' \\ j \neq j' \end{matrix} \quad (37)$$

with

$$\delta \hat{G}_4 = \frac{g}{\sqrt{2}m_W} \begin{pmatrix} 2m_b \delta m_b \tan \beta + 2m_t \delta m_t \cot \beta & \delta(m_b A_b) \tan \beta + \mu \delta m_b \\ \delta(m_t A_t) \cot \beta + \mu \delta m_t & 2(\delta m_t m_b + m_t \delta m_b) / \sin 2\beta \end{pmatrix}, \quad (38)$$

and analogously the expression for $\tilde{b}_i \rightarrow \tilde{t}_j H^-$ according to (13).

δm_q is the shift from the bare to the pole mass of the quark q and has two contributions (Fig. 1d). The gluon exchange contribution is

$$\delta m_q^{(g)} = -\frac{2}{3} \frac{\alpha_s}{\pi} m_q \left[B_0(m_q^2, 0, m_q^2) - B_1(m_q^2, 0, m_q^2) - r/2 \right], \quad (39)$$

and the gluino contribution is

$$\begin{aligned} \delta m_q^{(\tilde{g})} = & -\frac{\alpha_s}{3\pi} \left\{ m_q \left[B_1(m_q^2, m_{\tilde{g}}^2, m_{\tilde{q}_1}^2) + B_1(m_q^2, m_{\tilde{g}}^2, m_{\tilde{q}_2}^2) \right] \right. \\ & \left. + m_{\tilde{g}} \sin 2\theta_{\tilde{q}} \left[B_0(m_q^2, m_{\tilde{g}}^2, m_{\tilde{q}_1}^2) - B_0(m_q^2, m_{\tilde{g}}^2, m_{\tilde{q}_2}^2) \right] \right\}. \end{aligned} \quad (40)$$

The parameter r in Eq. (39) exhibits the dependence on the regularization scheme. As r does not cancel in the final result, we have to use dimensional reduction [12] ($r = 0$) which preserves supersymmetry at least at two-loop order.

For the renormalization of $m_q A_q$ we define the on-shell parameters $M_{\tilde{Q}, \tilde{U}, \tilde{D}}$ and $A_{t,b}$ in terms of squark pole masses $m_{\tilde{q}_i}$ and on-shell mixing angles $\theta_{\tilde{q}}$ (which will be defined below) using the tree-level relations (5) to (9). We thus get [11]

$$\delta(m_q A_q) = \frac{1}{2} (\delta m_{\tilde{q}_1}^2 - \delta m_{\tilde{q}_2}^2) \sin 2\theta_{\tilde{q}} + (m_{\tilde{q}_1}^2 - m_{\tilde{q}_2}^2) \cos 2\theta_{\tilde{q}} \delta\theta_{\tilde{q}} + \mu \{ \cot \beta, \tan \beta \} \delta m_q. \quad (41)$$

where again $\cot \beta$ ($\tan \beta$) is for $\tilde{q} = \tilde{t}$ (\tilde{b}). $\delta m_{\tilde{q}_i}^2$ is given by

$$\delta m_{\tilde{q}_i}^2 = \text{Re} \left[\Sigma_{ii}^{(g)}(m_{\tilde{q}_i}^2) + \Sigma_{ii}^{(\tilde{g})}(m_{\tilde{q}_i}^2) + \Sigma_{ii}^{(\tilde{q})}(m_{\tilde{q}_i}^2) \right] \quad (42)$$

with

$$\Sigma_{ii}^{(g)}(m_{\tilde{q}_i}^2) = -\frac{2}{3} \frac{\alpha_s}{\pi} m_{\tilde{q}_i}^2 \{ 2B_0(m_{\tilde{q}_i}^2, 0, m_{\tilde{q}_i}^2) + B_1(m_{\tilde{q}_i}^2, 0, m_{\tilde{q}_i}^2) \}, \quad (43)$$

$$\begin{aligned} \Sigma_{ii}^{(\tilde{g})}(m_{\tilde{q}_i}^2) = & -\frac{4}{3} \frac{\alpha_s}{\pi} \{ A_0(m_q^2) + m_{\tilde{q}_i}^2 B_1(m_{\tilde{q}_i}^2, m_{\tilde{g}}^2, m_q^2) \\ & + [m_{\tilde{g}}^2 + (-)^i m_{\tilde{g}} m_q \sin 2\theta_{\tilde{q}}] B_0(m_{\tilde{q}_i}^2, m_{\tilde{g}}^2, m_q^2) \}, \end{aligned} \quad (44)$$

$$\Sigma_{ii}^{(\tilde{q})}(m_{\tilde{q}_i}^2) = \frac{\alpha_s}{3\pi} \{ \cos^2 2\theta_{\tilde{q}} A_0(m_{\tilde{q}_i}^2) + \sin^2 2\theta_{\tilde{q}} A_0(m_{\tilde{q}_i'}^2) \}, \quad i \neq i'. \quad (45)$$

We also have to renormalize the squark mixing angle. This problem was first solved in [15]: there the counterterm $\delta\theta_{\tilde{q}}$ was fixed in the process $e^+e^- \rightarrow \tilde{q}_1 \tilde{q}_2$ such that it cancels the off-diagonal part of the squark wave-function corrections. $\delta\theta_{\tilde{q}} = \delta\theta_{\tilde{q}}^{(\tilde{q})} + \delta\theta_{\tilde{q}}^{(\tilde{g})}$ is thus given by

$$\delta\theta_{\tilde{q}}^{(\tilde{q})} = \frac{\alpha_s}{6\pi} \frac{\sin 4\theta_{\tilde{q}}}{m_{\tilde{q}_1}^2 - m_{\tilde{q}_2}^2} \left[A_0(m_{\tilde{q}_2}^2) - A_0(m_{\tilde{q}_1}^2) \right], \quad (46)$$

$$\delta\theta_{\tilde{q}}^{(\tilde{g})} = \frac{\alpha_s}{3\pi} \frac{m_{\tilde{g}} m_q}{I_{3L}^q(m_{\tilde{q}_1}^2 - m_{\tilde{q}_2}^2)} \left[B_0(m_{\tilde{q}_2}^2, m_{\tilde{g}}^2, m_q^2) \tilde{v}_{11} - B_0(m_{\tilde{q}_1}^2, m_{\tilde{g}}^2, m_q^2) \tilde{v}_{22} \right], \quad (47)$$

where \tilde{v}_{ij} comes from the $Z^0 \tilde{q}_i \tilde{q}_j^*$ couplings, $\tilde{v}_{11} = 4(I_{3L}^q \cos^2 \theta_{\tilde{q}} - s_W^2 e_q)$ and $\tilde{v}_{22} = 4(I_{3L}^q \sin^2 \theta_{\tilde{q}} - s_W^2 e_q)$ with $s_W^2 = \sin^2 \theta_W$. We will use this scheme in what follows. There are also other possibilities of defining the on-shell squark mixing angle. In [10], for instance, $\delta\theta_{\tilde{q}}$ was fixed such that the renormalized self-energy of the squarks remains diagonal on the \tilde{q}_1 mass shell. Similar conditions were used in [16, 17]. For comparison we list the counterterms $\delta\theta_{\tilde{q}}$ in these

schemes in terms of the squark self-energy Σ_{12} :

$$\begin{aligned}
\delta\theta_{\tilde{q}}([15]) &= \frac{1}{\tilde{v}_{11} - \tilde{v}_{22}} \frac{\text{Re} \left\{ \tilde{v}_{11} \Sigma_{12}(m_{\tilde{q}_2}^2) - \tilde{v}_{22} \Sigma_{12}(m_{\tilde{q}_1}^2) \right\}}{m_{\tilde{q}_1}^2 - m_{\tilde{q}_2}^2}, & (\text{used in this paper}) \\
\delta\theta_{\tilde{q}}([10]) &= \frac{\text{Re} \left\{ \Sigma_{12}(m_{\tilde{q}_1}^2) \right\}}{m_{\tilde{q}_1}^2 - m_{\tilde{q}_2}^2}, \\
\delta\theta_{\tilde{q}}(Q^2)([16]) &= \frac{\text{Re} \left\{ \Sigma_{12}(Q^2) \right\}}{m_{\tilde{q}_1}^2 - m_{\tilde{q}_2}^2}, \\
\delta\theta_{\tilde{q}}([17]) &= \frac{1}{2} \frac{\text{Re} \left\{ \Sigma_{12}(m_{\tilde{q}_1}^2) + \Sigma_{12}(m_{\tilde{q}_2}^2) \right\}}{m_{\tilde{q}_1}^2 - m_{\tilde{q}_2}^2}. & (48)
\end{aligned}$$

The differences between them are ultraviolet finite. In Fig. 2 we compare $\delta\theta_{\tilde{t}}$ of [10, 16, 17] to that of our scheme ([15]). As can be seen, the numerical differences between the various schemes are very small ($< 1\%$).

There is yet another subtlety that has to be taken into account: At tree-level and in the $\overline{\text{DR}}$ renormalization scheme $\text{SU}(2)_L$ symmetry requires that the parameter $M_{\tilde{Q}}$ in the \tilde{t} and \tilde{b} mass matrices have the same value. This is, however, not the case at loop-level in the on-shell scheme due to different shifts $\delta M_{\tilde{Q}}^2$ in the \tilde{t} and in the \tilde{b} sectors [11, 18]. In this paper we take $M_{\tilde{Q}}^2(\tilde{q}) = m_{\tilde{q}_1}^2 \cos^2 \theta_{\tilde{q}} + m_{\tilde{q}_2}^2 \sin^2 \theta_{\tilde{q}} - m_Z^2 \cos 2\beta (I_{3L}^q - e_q \sin^2 \theta_W) - m_q^2$ as the on-shell parameter in the \tilde{q} sector ($\tilde{q} = \tilde{t}, \tilde{b}$). This leads to a shift of $M_{\tilde{Q}}^2$ [11]:

$$M_{\tilde{Q}}^2(\tilde{b}) = M_{\tilde{Q}}^2(\tilde{t}) + \delta M_{\tilde{Q}}^2(\tilde{t}) - \delta M_{\tilde{Q}}^2(\tilde{b}) \quad (49)$$

with

$$\delta M_{\tilde{Q}}^2(\tilde{q}) = \delta m_{\tilde{q}_1}^2 \cos^2 \theta_{\tilde{q}} + \delta m_{\tilde{q}_2}^2 \sin^2 \theta_{\tilde{q}} - (m_{\tilde{q}_1}^2 - m_{\tilde{q}_2}^2) \sin 2\theta_{\tilde{q}} \delta\theta_{\tilde{q}} - 2m_q \delta m_q. \quad (50)$$

The underlying $\text{SU}(2)_L$ symmetry is reflected in the fact that the shift $\delta M_{\tilde{Q}}^2(\tilde{t}) - \delta M_{\tilde{Q}}^2(\tilde{b})$ is finite.

3.4 Real gluon emission

In order to cancel the infrared divergence we include the emission of real (hard and soft) gluons (Fig. 1e):

$$\delta\Gamma_{\text{real}} = \Gamma(\tilde{q}_i^\alpha \rightarrow \tilde{q}_j^\beta H_k g) = -\frac{\alpha_s |G_{ijk}^\alpha|^2}{3\pi^2 m_i} \left[I_0 + I_1 + m_i^2 I_{00} + m_j^2 I_{11} + X I_{01} \right]. \quad (51)$$

Again, $X = m_i^2 + m_j^2 - m_{H_k}^2$. The phase space integrals I_n , and I_{nm} have (m_i, m_j, m_{H_k}) as arguments and are given in [14].

We have checked explicitly that the corrected decay width Γ of Eq. (16) is ultraviolet and infrared finite.

4 Numerical results and discussion

Let us now turn to the numerical analysis. As input parameters we use $m_{\tilde{t}_1}$, $m_{\tilde{t}_2}$, $\cos\theta_{\tilde{t}}$, $\tan\beta$, μ , m_A , and $m_{\tilde{g}}$. From these we calculate the values of the soft SUSY-breaking parameters $M_{\tilde{Q}}(\tilde{t})$, $M_{\tilde{Q}}(\tilde{b})$, $M_{\tilde{U},\tilde{D}}$, and $A_{t,b}$ according to Eqs. (5) to (9) together with Eqs. (49) and (50), taking $M_{\tilde{D}} = 1.12 M_{\tilde{Q}}(\tilde{t})$ and $A_b = A_t$ for simplicity to fix the sbottom sector. Moreover, we take $m_t = 175$ GeV, $m_b = 5$ GeV, $m_Z = 91.2$ GeV, $\sin^2\theta_W = 0.23$, $\alpha(m_Z) = 1/129$, and $\alpha_s(m_Z) = 0.12$. For the running of α_s we use $\alpha_s(Q) = 12\pi/[(33 - 2n_f)\ln(Q^2/\Lambda_{n_f}^2)]$ with n_f the number of quark flavors. We take $\alpha_s = \alpha_s(m_{\tilde{q}_i^\alpha})$ for the \tilde{q}_i^α decay except for the shift in Eqs. (49) and (50) for which we take $\alpha_s = \alpha_s(M_{\tilde{Q}}(\tilde{t}))$. For the radiative corrections to the h^0 and H^0 masses and their mixing angle α ($-\frac{\pi}{2} \leq \alpha < \frac{\pi}{2}$ by convention) we use the formulae of [19]²; for those to m_{H^+} we follow [20]. In order to respect the experimental mass bounds from LEP2 [21] and Tevatron [22] we impose $m_{h^0} > 90$ GeV, $m_{\tilde{t}_1,\tilde{b}_1} > 85$ GeV, and $m_{\tilde{g}} > 300$ GeV. Moreover, we require $\delta\rho(\tilde{t} - \tilde{b}) < 0.0012$ [23] from electroweak precision measurements using the one-loop formulae of [24] and $A_t^2 < 3(M_{\tilde{Q}}^2(\tilde{t}) + M_{\tilde{U}}^2 + m_{H_2}^2)$, $A_b^2 < 3(M_{\tilde{Q}}^2(\tilde{b}) + M_{\tilde{D}}^2 + m_{H_1}^2)$ with $m_{H_2}^2 = (m_A^2 + m_Z^2)\cos^2\beta - \frac{1}{2}m_Z^2$ and $m_{H_1}^2 = (m_A^2 + m_Z^2)\sin^2\beta - \frac{1}{2}m_Z^2$ [25] from tree-level vacuum stability.

As a reference point we take $m_{\tilde{t}_1} = 250$ GeV, $m_{\tilde{t}_2} = 600$ GeV, $\cos\theta_{\tilde{t}} = 0.26$ ($\theta_{\tilde{t}} \simeq 75^\circ$), $\tan\beta = 3$, $\mu = 550$ GeV, $m_A = 150$ GeV, and $m_{\tilde{g}} = 600$ GeV. This leads to $m_{\tilde{b}_1} = 564$ GeV³, $m_{\tilde{b}_2} = 627$ GeV, $\cos\theta_{\tilde{b}} = 0.99$, $A_{t,b} = -243$ GeV, $m_{h^0} = 100$ GeV, $m_{H^0} = 162$ GeV, $\sin\alpha = -0.58$, and $m_{H^+} = 164$ GeV. Thus \tilde{t}_2 can decay into $\tilde{t}_1 + (h^0, H^0, A^0)$, and $\tilde{b}_{1,2}$ can decay into $\tilde{t}_1 H^-$.

We first discuss the parameter dependence of the widths of \tilde{t}_2 decays into neutral Higgs bosons by varying one of the input parameters of the reference point. We define the SUSY-QCD corrections as the difference between the corrected width Γ of Eq. (16) and the tree-level width Γ^0 of Eq. (14).

Figure 3 shows the tree-level and the SUSY-QCD corrected widths of the decays $\tilde{t}_2 \rightarrow \tilde{t}_1 + (h^0, H^0, A^0)$ as a function of $m_{\tilde{t}_2}$. The relative corrections $\delta\Gamma/\Gamma^0 \equiv (\Gamma - \Gamma^0)/\Gamma^0$ are about -10% for the decay into h^0 and -9% to -62% for the decay into A^0 . The corrections for $\tilde{t}_2 \rightarrow \tilde{t}_1 H^0$ are -9% , -45% , and $+45\%$ for $m_{\tilde{t}_2} = 420, 670$, and 900 GeV, respectively. The spikes in the corrected decay widths for $m_{\tilde{t}_2} = 775$ GeV are due to the $\tilde{t}_2 \rightarrow t\tilde{g}$ threshold. The different shapes of the decay widths can be understood by the wide range of the parameters entering the Higgs couplings to stops. In the range $m_{\tilde{t}_2} = 300$ GeV to 900 GeV, we have $A_t = 144$ GeV to -889 GeV and $\sin\alpha = -0.52$ to -0.73 ($m_{h^0} = 81$ GeV to 114 GeV, and $m_{H^0} = 163$ GeV to 170 GeV).

Figure 4 shows the $\cos\theta_{\tilde{t}}$ dependence of the tree-level and the corrected widths of $\tilde{t}_2 \rightarrow \tilde{t}_1 + (h^0, H^0, A^0)$ decays. Again the shapes of the decay widths reflect their dependence on the

²Notice that [19, 20] have the opposite sign convention for the parameter μ .

³Notice that at tree-level one has $m_{\tilde{b}_1} = 560$ GeV because $M_{\tilde{Q}} = 558$ GeV for both the \tilde{t} and \tilde{b} mass matrices; at $\mathcal{O}(\alpha_s)$, however, one gets $M_{\tilde{Q}}(\tilde{t}) = 558$ GeV and $M_{\tilde{Q}}(\tilde{b}) = 563$ GeV.

underlying SUSY parameters in a characteristic way. In particular we have $A_t = 1033, 183, -666$ GeV and $\sin \alpha = -0.748, -0.565, -0.726$ for $\cos \theta_{\tilde{t}} = -0.7, 0, 0.7$, respectively. Apart from the points where the tree-level decay amplitudes vanish the relative corrections range from -40% to 20% .

In Fig. 5 we show the tree-level and the SUSY-QCD corrected decay widths as a function of m_A . For $m_A = 100, 200, 300$ GeV we have $m_{h^0} = 85, 104, 105$ GeV, $m_{H^0} = 128, 207, 304$ GeV, and $\sin \alpha = -0.87, -0.45, -0.37$, respectively. The corrections to $\Gamma^0(\tilde{t}_2 \rightarrow \tilde{t}_1 h^0)$ range from -15% to -7% for $m_A = 100$ GeV to 400 GeV. Those to $\Gamma^0(\tilde{t}_2 \rightarrow \tilde{t}_1 H^0)$ are -50% to -22% for $m_A \gtrsim 114$ GeV, and those to $\Gamma^0(\tilde{t}_2 \rightarrow \tilde{t}_1 A^0)$ are about -25% .

As for the dependence on the gluino mass, as can be seen in Fig. 6, the gluino decouples very slowly: in the range $m_{\tilde{g}} = 300$ GeV to 1500 GeV $\delta\Gamma/\Gamma^0$ varies from $(-9\%, -37\%, -28\%)$ to $(-7\%, -16\%, -14\%)$ for the decays $\tilde{t}_2 \rightarrow \tilde{t}_1 + (h^0, H^0, A^0)$, apart from the $\tilde{t}_2 \rightarrow t\tilde{g}$ threshold at $m_{\tilde{g}} = 425$ GeV.

As for the dependence on $\tan \beta$, we get $\Gamma(\tilde{t}_2 \rightarrow \tilde{t}_1 h^0) = 2.68, 2.09, 1.42$ GeV with $\delta\Gamma/\Gamma^0 \simeq -10\%, -7\%, -5\%$ for $\tan \beta = 3, 10, 30$, respectively. Likewise, we get $\Gamma = 0.67, 1.61, 2.45$ GeV with $\delta\Gamma/\Gamma^0 \simeq -27\%, -19\%, -17\%$ for the decay into H^0 and $\Gamma = 2.1, 2.64, 2.92$ GeV with $\delta\Gamma/\Gamma^0 \simeq -22\%, -19\%, -18\%$ for the decay into A^0 , respectively.

Let us now turn to the sbottom decays. We start again from the reference point given above. For the decay $\tilde{b}_1 \rightarrow \tilde{t}_1 H^-$ we get $\Gamma = 3.88$ GeV with $\delta\Gamma/\Gamma^0 = -24\%$, and for the decay $\tilde{b}_2 \rightarrow \tilde{t}_1 H^-$ we get $\Gamma = 0.08$ GeV with $\delta\Gamma/\Gamma^0 = +87\%$. As in our examples the width of the latter decay is usually quite small (because $\tilde{b}_2 \simeq \tilde{b}_R$ and $\tilde{t}_1 \sim \tilde{t}_R$) we will discuss only the parameter dependence of the \tilde{b}_1 decay.

Figure 7 shows the tree-level and the SUSY-QCD corrected widths of this decay as a function of $m_{\tilde{t}_1}$. The SUSY-QCD corrections are about -25% . Notice that at tree-level we have $m_{\tilde{b}_1} = 556$ GeV to 566 GeV for $m_{\tilde{t}_1} = 85$ GeV to 400 GeV, whereas at $\mathcal{O}(\alpha_s)$ we have $m_{\tilde{b}_1} = 561$ GeV to 570 GeV. Therefore, the thresholds at tree-level and one-loop level are slightly different.

The dependence on the stop mixing angle is shown in Fig. 8 for $\tan \beta = 3$ and 10 , and the other parameters as given above. (For $|\cos \theta_{\tilde{t}}| \gtrsim 0.72$ the decay $\tilde{b}_1 \rightarrow \tilde{t}_1 H^-$ is kinematically not allowed.) In case of $\tan \beta = 3$, the SUSY-QCD corrections range from about -40% to 26% , with $\delta\Gamma/\Gamma^0 > 0$ for $\cos \theta_{\tilde{t}} \lesssim -0.6$. In case of $\tan \beta = 10$ $\delta\Gamma/\Gamma^0$ is much larger. For $\cos \theta_{\tilde{t}} \gtrsim 0.5$ and $\tan \beta = 10$ we even get a negative corrected decay width. This is mainly due to a large contribution stemming from the term $\delta(m_b A_b) \sim \mu \tan \beta \delta m_b$ of Eq. (41) and was already mentioned in [11]. The same problem can occur for the decays $\tilde{b}_2 \rightarrow \tilde{b}_1 + (h^0, H^0, A^0)$ and $\tilde{t}_2 \rightarrow \tilde{b}_1 H^+$ which may be important for large $\tan \beta$ (due to the large bottom Yukawa coupling and the large \tilde{b}_1 - \tilde{b}_2 mass splitting).

We have also studied the dependence on m_A . In the case $\tan \beta = 3$ (10) we have found that $\delta\Gamma/\Gamma^0(\tilde{b}_1 \rightarrow \tilde{t}_1 H^-) \sim -20\%$ (-40%) for $m_A = 100$ GeV to 285 GeV and the other parameters as given above.

As for the dependence on the gluino mass, $\delta\Gamma/\Gamma^0(\tilde{b}_1 \rightarrow \tilde{t}_1 H^-)$ ranges from -26% to -14% (-47% to -39%) for $m_{\tilde{g}} = 300$ GeV to 1500 GeV and $\tan \beta = 3$ (10).

In [10] a numerical analysis for the decays $\tilde{t}_2 \rightarrow \tilde{t}_1 + (h^0, A^0)$ was made. Whereas we agree with their figure for $\tilde{t}_2 \rightarrow \tilde{t}_1 A^0$, we find a difference of about 10% in both the tree-level and

the corrected widths of $\tilde{t}_2 \rightarrow \tilde{t}_1 h^0$. This may be due to a different treatment of the radiative corrections to the h^0 mass and mixing angle α .⁴

5 Conclusions

We have calculated the $\mathcal{O}(\alpha_s)$ SUSY–QCD corrections to the decay widths of $\tilde{q}_2 \rightarrow \tilde{q}_1 + (h^0, H^0, A^0)$ and $\tilde{q}_i \rightarrow \tilde{q}'_j H^\pm$ ($\tilde{q} = \tilde{t}, \tilde{b}$) in the on-shell scheme. We have taken into account appropriate shifts for the soft SUSY–breaking parameters defined in terms of on-shell squark masses and mixing angles. It has turned out that the SUSY–QCD corrections are mostly negative and of the order of a few ten percent and should therefore be taken into account.

Acknowledgements

The work of A.B., H.E., S.K., W.M., and W.P. was supported by the ‘‘Fonds zur F6orderung der wissenschaftlichen Forschung’’ of Austria, project no. P10843–PHY. The work of Y.Y. was supported in part by the Grant–in–aid for Scientific Research from the Ministry of Education, Science, and Culture of Japan, No. 10740106, and by Fuuju–kai Foundation.

Appendix: Squark – Squark – Higgs Couplings

(a) squark – squark – h^0

$$\hat{G}_1^{\tilde{q}} = \begin{pmatrix} \frac{g m_Z}{c_W} C_L s_{\alpha+\beta} - \sqrt{2} m_q h_q \begin{Bmatrix} c_\alpha \\ -s_\alpha \end{Bmatrix} & -\frac{1}{\sqrt{2}} h_q (A_q \begin{Bmatrix} c_\alpha \\ -s_\alpha \end{Bmatrix} + \mu \begin{Bmatrix} s_\alpha \\ -c_\alpha \end{Bmatrix}) \\ -\frac{1}{\sqrt{2}} h_q (A_q \begin{Bmatrix} c_\alpha \\ -s_\alpha \end{Bmatrix} + \mu \begin{Bmatrix} s_\alpha \\ -c_\alpha \end{Bmatrix}) & \frac{g m_Z}{c_W} C_R s_{\alpha+\beta} - \sqrt{2} m_q h_q \begin{Bmatrix} c_\alpha \\ -s_\alpha \end{Bmatrix} \end{pmatrix} \quad (52)$$

for $\begin{Bmatrix} \text{up} \\ \text{down} \end{Bmatrix}$ type squarks respectively. We use the abbreviations $c_W = \cos \theta_W$, $s_\alpha = \sin \alpha$, $c_\alpha = \cos \alpha$, $s_{\alpha+\beta} = \sin(\alpha+\beta)$, $C_L = I_{3L}^q - e_q \sin^2 \theta_W$, and $C_R = e_q \sin^2 \theta_W$. α is the mixing angle in the CP even neutral Higgs boson sector. h_q are the Yukawa couplings:

$$h_t = \frac{g m_t}{\sqrt{2} m_W \sin \beta}, \quad h_b = \frac{g m_b}{\sqrt{2} m_W \cos \beta}. \quad (53)$$

⁴We thank A. Djouadi and W. Hollik for correspondence on this point.

(b) squark – squark – H^0

$$\hat{G}_2^{\tilde{q}} = \begin{pmatrix} -\frac{g m_Z}{c_W} C_L c_{\alpha+\beta} - \sqrt{2} m_q h_q \begin{Bmatrix} s_\alpha \\ c_\alpha \end{Bmatrix} & -\frac{1}{\sqrt{2}} h_q (A_q \begin{Bmatrix} s_\alpha \\ c_\alpha \end{Bmatrix} - \mu \begin{Bmatrix} c_\alpha \\ s_\alpha \end{Bmatrix}) \\ -\frac{1}{\sqrt{2}} h_q (A_q \begin{Bmatrix} s_\alpha \\ c_\alpha \end{Bmatrix} - \mu \begin{Bmatrix} c_\alpha \\ s_\alpha \end{Bmatrix}) & -\frac{g m_Z}{c_W} C_R c_{\alpha+\beta} - \sqrt{2} m_q h_q \begin{Bmatrix} s_\alpha \\ c_\alpha \end{Bmatrix} \end{pmatrix} \quad (54)$$

(c) squark – squark – A^0

$$\hat{G}_3^{\tilde{q}} = i \frac{g m_q}{2 m_W} \begin{pmatrix} 0 & -A_q \begin{Bmatrix} \cot \beta \\ \tan \beta \end{Bmatrix} - \mu \\ A_q \begin{Bmatrix} \cot \beta \\ \tan \beta \end{Bmatrix} + \mu & 0 \end{pmatrix} \quad (55)$$

(d) squark – squark – H^\pm

$$\hat{G}_4 = \frac{g}{\sqrt{2} m_W} \begin{pmatrix} m_b^2 \tan \beta + m_t^2 \cot \beta - m_W^2 \sin 2\beta & m_b (A_b \tan \beta + \mu) \\ m_t (A_t \cot \beta + \mu) & \frac{2 m_t m_b}{\sin 2\beta} \end{pmatrix} \quad (56)$$

References

- [1] J. Ellis and S. Rudaz, Phys. Lett. B 128 (1983) 248;
J. F. Gunion and H. E. Haber, Nucl. Phys. B 272 (1986) 1; B402 (1993) 567 (E).
- [2] A. Bartl, W. Majerotto and W. Porod, Z. Phys. C 64 (1994) 499; C 68 (1995) 518 (E).
- [3] H. E. Haber and G. L. Kane, Phys. Rep. 117 (1985) 75.
- [4] A. Bartl, H. Eberl, K. Hidaka, S. Kraml, T. Kon, W. Majerotto, W. Porod and Y. Yamada, Phys. Lett. B 435 (1998) 118.
- [5] S. Kraml, H. Eberl, A. Bartl, W. Majerotto and W. Porod, Phys. Lett. B 386 (1996) 175.
- [6] A. Djouadi, W. Hollik and C. Jünger, Phys. Rev. D 55 (1997) 6975.
- [7] W. Beenakker, R. Höpker, T. Plehn and P. M. Zerwas, Z. Phys. C 75 (1997) 349.
- [8] W. Beenakker, R. Höpker and P. M. Zerwas, Phys. Lett. B 378 (1996) 159.
- [9] A. Bartl, H. Eberl, K. Hidaka, S. Kraml, W. Majerotto, W. Porod and Y. Yamada, Phys. Lett. B 419 (1998) 243.
- [10] A. Arhrib, A. Djouadi, W. Hollik and C. Jünger, Phys. Rev. D 57 (1998) 5860.

- [11] A. Bartl, H. Eberl, K. Hidaka, T. Kon, W. Majerotto and Y. Yamada, Phys. Lett. B 402 (1997) 303.
- [12] W. Siegel, Phys. Lett. B 84 (1979) 193;
D. M. Capper, D. R. T. Jones and P. van Nieuwenhuizen, Nucl. Phys. B 167 (1980) 479;
I. Jack, D. R. T. Jones, S. P. Martin and Y. Yamada, Phys. Rev. D 50 (1994) 5481;
I. Jack and D. R. T. Jones, hep-ph/9707278.
- [13] G. Passarino and M. Veltman, Nucl. Phys. B 160 (1979) 151.
- [14] A. Denner, Fortschr. Phys. 41 (1993) 307.
- [15] H. Eberl, A. Bartl and W. Majerotto, Nucl. Phys. B 472 (1996) 481.
- [16] W. Beenakker, R. Höpker, T. Plehn and P. M. Zerwas, Z. Phys. C 75 (1997) 349.
- [17] J. Guasch, J. Sola and W. Hollik, Phys. Lett. B 437 (1998) 88.
- [18] Y. Yamada, Phys. Rev. D54 (1996) 1150.
- [19] J. Ellis, G. Ridolfi and F. Zwirner, Phys. Lett. B 262 (1991) 477.
- [20] A. Brignole, Phys. Lett. B 277 (1992) 313.
- [21] E. Lancon (ALEPH), V. Ruhlmann-Kleider (DELPHI), R. Clare (L3) and D. Plane (OPAL), talks at the 50th CERN LEPC meeting, 12 Nov. 1998; for minutes and transparencies, see <http://www.cern.ch/Committees/LEPC/minutes/LEPC50.html>
- [22] DØ Collab., S. Abachi et al., Phys. Rev. Lett. 75 (1995) 618; Phys. Rev. Lett 76 (1996) 2222;
CDF Collab., F. Abe et al., Phys. Rev. D 56 (1997) 1357.
J. A. Valls, talk at ICHEP98, FEERMILAB-Conf-98-292-E.
- [23] G. Altarelli, R. Barbieri and F. Caravaglios, Int. J. Mod. Phys. A13 (1998) 1031.
- [24] M. Drees and K. Hagiwara, Phys. Rev. D42 (1990) 1709.
- [25] J. P. Derendinger and C. A. Savoy, Nucl. Phys. B237 (1984) 307.

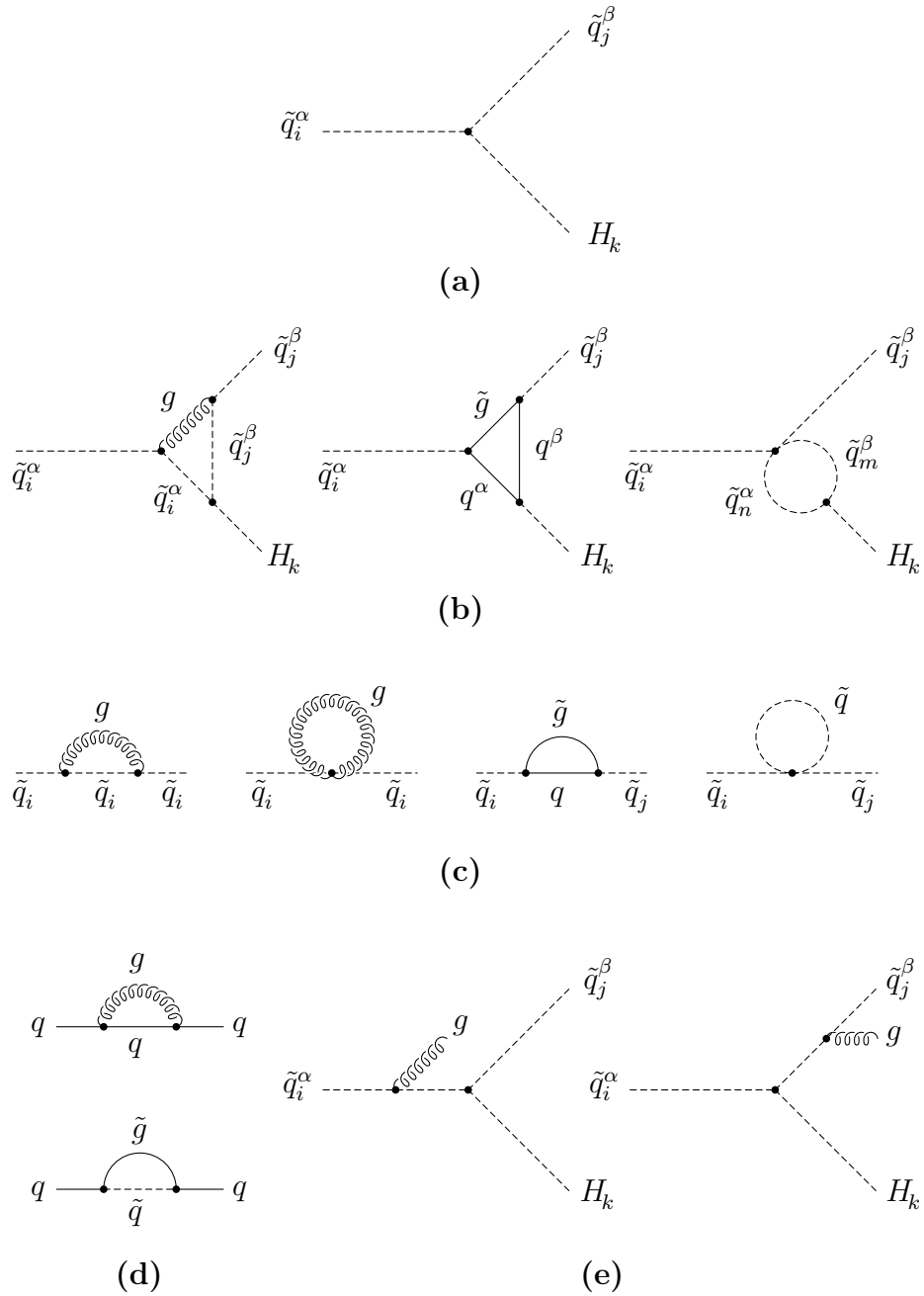


Figure 1: Feynman diagrams relevant for the $\mathcal{O}(\alpha_s)$ SUSY-QCD corrections to squark decays into Higgs bosons.

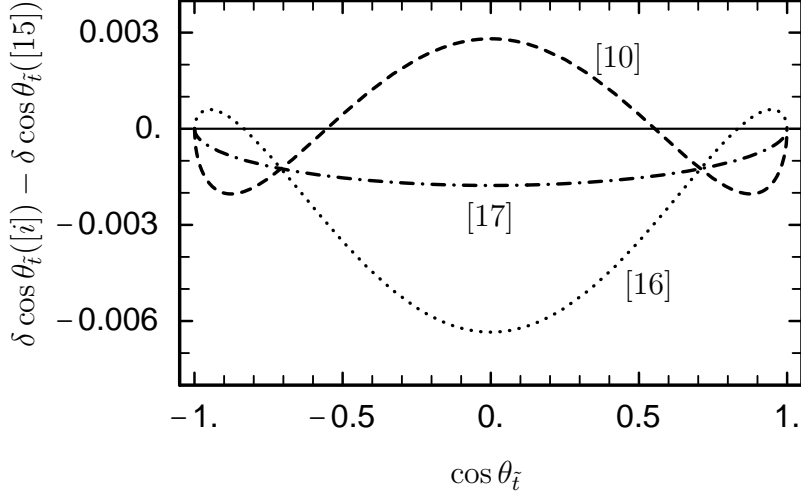


Figure 2: Differences in $\delta \cos \theta_{\tilde{t}}$ between [10, 16, 17] and our scheme [15] as a function of $\cos \theta_{\tilde{t}}$, for $m_{\tilde{t}_1} = 250$ GeV, $m_{\tilde{t}_2} = 600$ GeV, and $m_{\tilde{g}} = 600$ GeV. For $\delta \cos \theta_{\tilde{t}}(Q^2)$ ([16]) we have taken $Q^2 = m_{\tilde{t}_2}^2$.

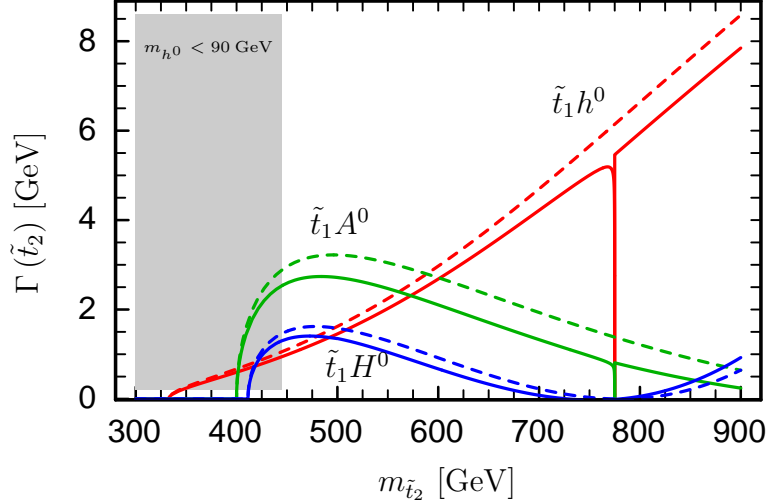


Figure 3: Tree-level (dashed lines) and $\mathcal{O}(\alpha_s)$ SUSY-QCD corrected (solid lines) decay widths of $\tilde{t}_2 \rightarrow \tilde{t}_1 + (h^0, H^0, A^0)$ as a function of $m_{\tilde{t}_2}$, for $m_{\tilde{t}_1} = 250$ GeV, $\cos \theta_{\tilde{t}} = 0.26$, $\mu = 550$ GeV, $\tan \beta = 3$, $m_A = 150$ GeV, and $m_{\tilde{g}} = 600$ GeV. The grey area is excluded by the bound $m_{h^0} > 90$ GeV.

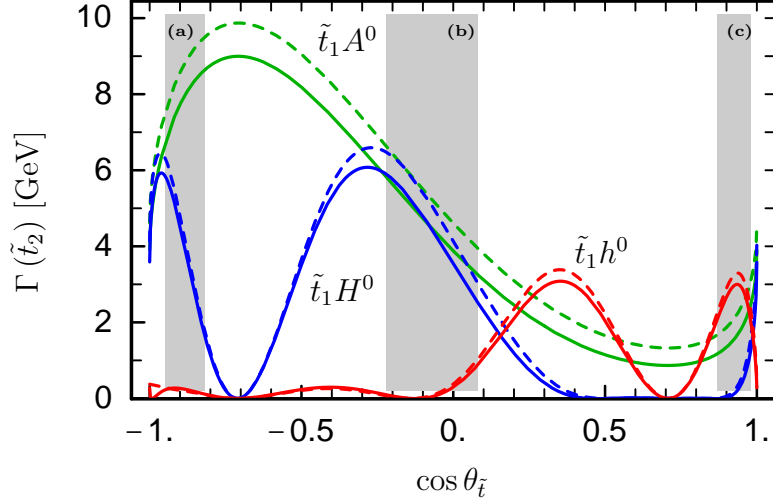


Figure 4: Tree-level (dashed lines) and $\mathcal{O}(\alpha_s)$ SUSY-QCD corrected (solid lines) decay widths of $\tilde{t}_2 \rightarrow \tilde{t}_1 + (h^0, H^0, A^0)$ as a function of $\cos \theta_{\tilde{t}}$, for $m_{\tilde{t}_1} = 250 \text{ GeV}$, $m_{\tilde{t}_2} = 600 \text{ GeV}$, $\mu = 550 \text{ GeV}$, $\tan \beta = 3$, $m_A = 150 \text{ GeV}$, and $m_{\tilde{g}} = 600 \text{ GeV}$. The grey areas are excluded by the constraints given in the text: $\delta\rho(\tilde{t}-\tilde{b}) > 0.0012$ in (a), $m_{h^0} < 90 \text{ GeV}$ in (b), and unstable vacuum in (c).

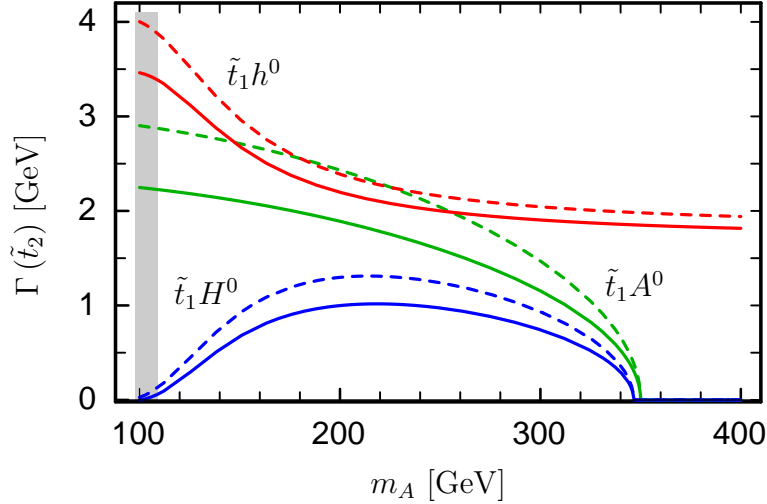


Figure 5: Tree-level (dashed lines) and $\mathcal{O}(\alpha_s)$ SUSY-QCD corrected (solid lines) decay widths of $\tilde{t}_2 \rightarrow \tilde{t}_1 + (h^0, H^0, A^0)$ as a function of m_A , for $m_{\tilde{t}_1} = 250 \text{ GeV}$, $m_{\tilde{t}_2} = 600 \text{ GeV}$, $\cos \theta_{\tilde{t}} = 0.26$, $\mu = 550 \text{ GeV}$, $\tan \beta = 3$, and $m_{\tilde{g}} = 600 \text{ GeV}$. The grey area is excluded by the bound $m_{h^0} > 90 \text{ GeV}$.

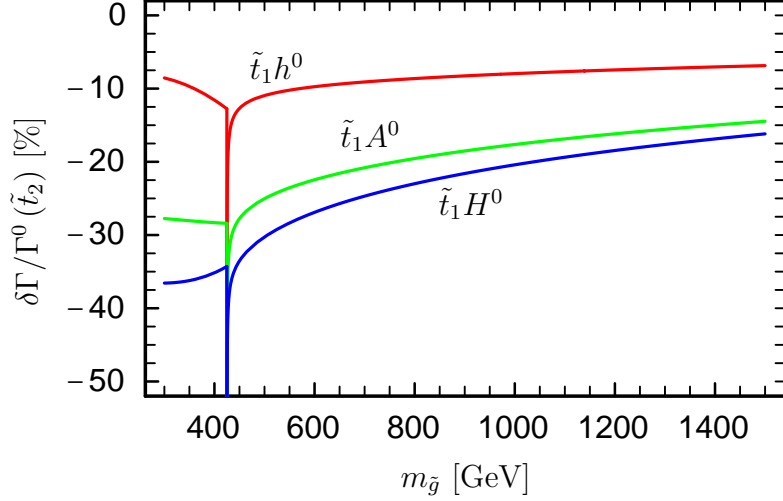


Figure 6: $\mathcal{O}(\alpha_s)$ SUSY–QCD corrections (in %) to the widths of $\tilde{t}_2 \rightarrow \tilde{t}_1 + (h^0, H^0, A^0)$ as a function of $m_{\tilde{g}}$, for $m_{\tilde{t}_1} = 250$ GeV, $m_{\tilde{t}_2} = 600$ GeV, $\cos\theta_{\tilde{t}} = 0.26$, $\mu = 550$ GeV, $\tan\beta = 3$, and $m_A = 150$ GeV.

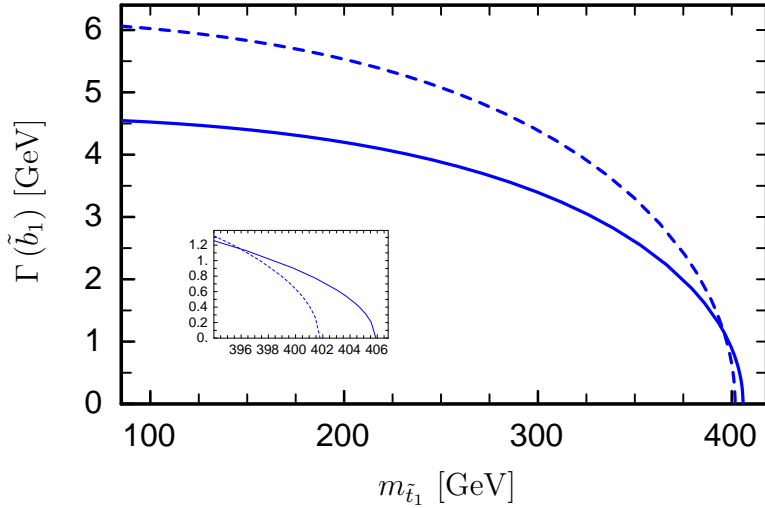


Figure 7: Tree–level (dashed line) and $\mathcal{O}(\alpha_s)$ SUSY–QCD corrected (solid line) decay widths of $\tilde{b}_1 \rightarrow \tilde{t}_1 H^-$ as a function of $m_{\tilde{t}_1}$, for $m_{\tilde{t}_2} = 600$ GeV, $\cos\theta_{\tilde{t}} = 0.26$, $\mu = 550$ GeV, $\tan\beta = 3$, $m_A = 150$ GeV, and $m_{\tilde{g}} = 600$ GeV. The insert zooms on the different thresholds at tree– and one–loop level.

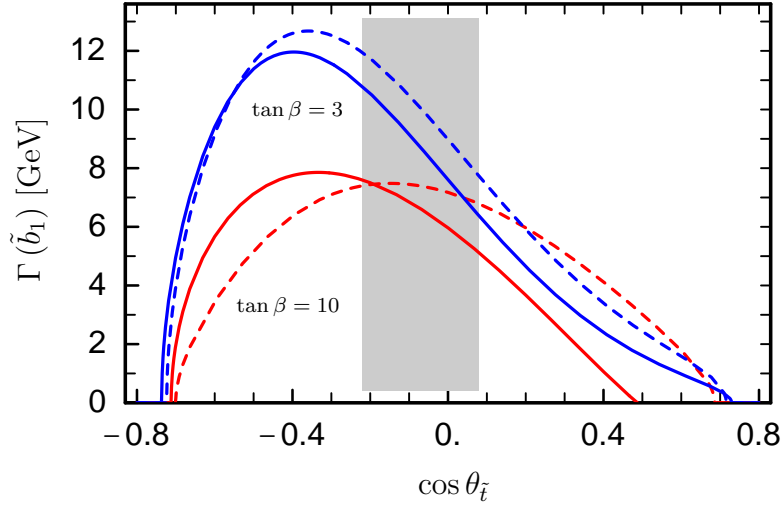


Figure 8: Tree-level (dashed lines) and $\mathcal{O}(\alpha_s)$ SUSY-QCD corrected (solid lines) decay widths of $\tilde{b}_1 \rightarrow \tilde{t}_1 H^-$ as a function of $\cos \theta_{\tilde{t}}$, for $m_{\tilde{t}_1} = 250$ GeV, $m_{\tilde{t}_2} = 600$ GeV, $\mu = 550$ GeV, $m_A = 150$ GeV, $m_{\tilde{g}} = 600$ GeV, and $\tan \beta = 3, 10$. The grey area is excluded for $\tan \beta = 3$ by the bound $m_{\tilde{t}_0} > 90$ GeV.